Compton scattering of photons from electrons bound in light elements

P. M. Bergstrom, Jr.

Department of Physics and Astronomy, University of Tennessee, Knoxville, Tennessee 37996 and Oak Ridge National Laboratory, Oak Ridge, Tennessee 37831

Abstract

A brief introduction to the topic of Compton scattering from bound electrons is presented. The fundamental nature of this process in understanding quantum phenomena is reviewed. Methods for accurate theoretical evaluation of the Compton scattering cross section are presented. Examples are presented for scattering of several keV photons from helium.

Samson, Greene and Bartlett[1] have recently noted that experiments measuring the ratio of double to single ionization by single photon impact on helium[2] are dominated at several keV by Compton scattering. Andersson and Burgdörfer[3] have estimated the contribution of Compton scattering to this ratio; relying on photoionization and shakeoff data. We discuss the nature of the bound Compton scattering and consider methods to obtain total cross sections for this process.

Compton scattering has been a valuable test of the most fundamental ideas of modern physics. Arthur Holly Compton observed that radiation scattered from atoms consists of essentially two components; the first at the wavelength of the incident radiation, corresponding to classical scattering, and the rest at a wavelength which varies with scattering angle. The inelastically scattered component may be roughly understood as scattering from free stationary electrons. The kinematics of Compton scattering from free stationary charges is readily determined from relativistic energy and momentum conservation under the further assumption that the radiation is quantized according to Planck's law and that these light quanta (or photons) and the target interact. The energy of the scattered radiation is uniquely determined by the energy of the incident radiation and by the scattering angle as

$$\omega_c = \frac{\omega_i}{1 + \frac{\omega_i}{mc^2}(1 - cos\theta)} \tag{1}$$

This result (actually the analogous result for the shift in wavelength) was derived independently and published nearly simultaneously by Compton[4] and Debye[5] and depends on a quantal or particlelike description of radiation.

Shortly after the development of the wave mechanical description of atomic phenomena, DuMond[6] suggested that Compton scattering could be used to distinguish between various atomic models. While radiation scattered from atoms approximately satisfies Eq.(1) , the free Compton line (peak) which is observed in the spectrum of scattered energies at fixed angle is somewhat broadened. Dumond related this broadening to the momentum distribution of the bound electrons. He tried a number of different trial momentum distributions for the different electronic states, finding agreement between the observed spectrum, for scattering of Mo K_α radiation from beryllium, and a model that used the free atom wave mechanical predictions for the inner shell electrons and the free electron Sommerfeld model for the valence electrons.

DuMond's relationship between the momentum distribution of the bound electrons and the Compton scattering cross section has since been more rigorously established within the impulse approximation[7-11]. This relationship makes Compton scattering a unique tool for investigating all aspects of the bound charge distribution, including correlations. In the remainder of this paper, we discuss the nature of the Compton scattering process and methods for calculating cross-sections. We concentrate on the accurate, efficient evaluation of the cross-section for scattering of high energy photons from helium.

The lowest order amplitude for Compton scattering may be obtained by evaluating the diagrams of Fig. 1 within external field quantum electrodynamics. Such calculations have recently been accomplished[12,13]. As a result, it is now possible to understand the region of validity of simpler, more approximate approaches. The features of the scattered photon spectrum, at fixed scattering angle, are apparent in the nonrelativistic Kramers Heisenberg Waller (KHW)[14] matrix element. In the Coulomb gauge the KHW matrix element is written

$$\begin{aligned} \mathrm{M}_{KHW} = {} & \left(\epsilon_1 \cdot \epsilon_2^*\right) \left\langle f \left| e^{i(\mathbf{k}_1 - \mathbf{k}_2)\cdot \mathbf{r}} \right| i \right\rangle - \sum_n \frac{\left\langle f \left| e^{-i\mathbf{k}_2 \cdot \mathbf{r}} \left(\epsilon_2^* \cdot \mathbf{p}\right) \right| n \right\rangle \left\langle n \left| e^{i\mathbf{k}_1 \cdot \mathbf{r}} \left(\epsilon_1 \cdot \mathbf{p}\right) \right| i \right\rangle}{E_n - (E_B + \omega_1 + i\epsilon)} \\ & - \sum_n \frac{\left\langle f \left| e^{i\mathbf{k}_1 \cdot \mathbf{r}} \left(\epsilon_1 \cdot \mathbf{p}\right) \right| n \right\rangle \left\langle n \left| e^{-i\mathbf{k}_2 \cdot \mathbf{r}} \left(\epsilon_2^* \cdot \mathbf{p}\right) \right| i \right\rangle}{E_n - (E_B - \omega_2)} \end{aligned} \tag{2}$$

where ϵ_1 and ϵ_2 are the polarization vectors for the incident and scattered photons, $\mathbf{k}_1$ and $\mathbf{k}_2$ are the incident and scattered photon momenta, ω_1 and ω_2 are the incident and scattered photon energies, $|i\rangle$, $|f\rangle$ and $|n\rangle$ are the electron wave functions and where E_B is the binding energy of the scattering electron. The first term A^2 or seagull term) of the KHW matrix element accounts for the Compton peak. The remaining terms, called the **p•A** or pole terms, give divergent behavior for soft scattered photons in all shells and resonant behavior in the outer atomic shells. *S* matrix calculations contain all three features. Fig. 2 presents a case, the scattering of 279 keV photons from the L3 subshell of lead, where all three features are observed. The dominant features are the angle dependent Compton peak in the hard photon region of the spectrum and the nearly isotropic resonance at the K-L3 characteristic energy. The divergent soft scattered photon spectrum is also seen.

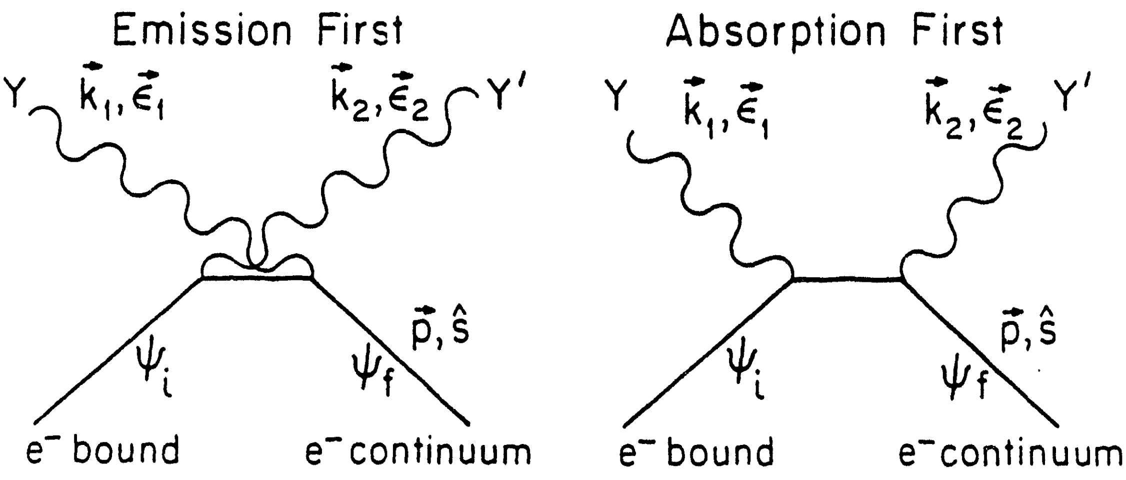

Figure 1. *Diagrams representing the S matrix amplitudes which must be evaluated to obtain the Compton scattering matrix element.*

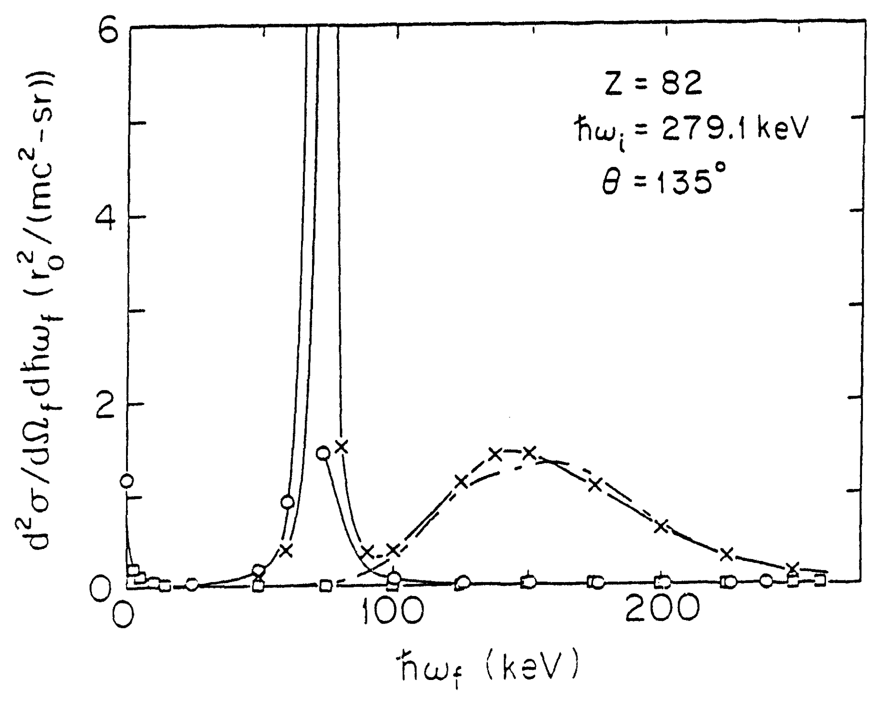

Figure 2. *Comparison of various nonrelativistic calculations with the it S matrix calculation (solid line) for the scattering of 279 keV photons from the L3 subshell of lead.*

The validity of the A^2 approximation in describing the peak region of the double differential cross section, for high photon energies, has been discussed by Eisenberger and Platzmann[7]. Comparing their experimental data for the scattering of 17.4 keV photons from helium, they found that the Compton peak is well described using only this term. The validity of the A^2 approximation in scattering from the K shell for any incident photon energy and scattering angle may be simply understood in terms of the underlying kinematics. We illustrate this in Fig. 3. The maximum scattered photon energy, the kinematic limit for the process, is determined by energy conservation to be the incident photon energy minus the binding energy of the scattering electron. In order for the Compton peak to be observable, it must shift to kinematically allowed energies. The shift for bound electron scattering is approximately equal to the free Compton shift to lower energies plus the Compton defect ($\approx E_B / 6$) to higher energies. Bergstrom et al[13] have derived the following expression for the incident photon energy at which the center of the peak is observable for any scattering angle

$$\omega_1 > \sqrt{\frac{7}{3\,(1-cos\theta)}\frac{E_B}{Z\alpha}}. \tag{3}$$

For incident photon energies that satisfy Eq. (3), the A^2 term is usually dominant and approximations derived from it are adequate.

The most common A^2 treatments involve direct evaluation of the matrix element or the impulse approximation discussed above. It is evident from Eq. (2) that a direct evaluation of the A^2 term necessarily involves retaining higher multiples as the usual electric dipole approximation vanishes. In Fig. 4, the A^2 approximation to the cross section singly differential in scattered photon angle is given along with the multipole contributions for the scattering of 12 keV photons from the K shell of helium. The need for many multipoles to accurately describe the spectrum is clear, particularly near the the scattered photon energy of 11.46 keV, which corresponds to the energy predicted by Eq. (1) when θ= 180 degrees. Another interesting feature is the possibility of ejection of the electron into an s state. This zero-zero transition, strictly forbidden in a nonrelativistic formalism for single photon processes, is possible because Compton scattering is a two photon process and the angular momentum of the incident photon can be completely transferred to the scattered photon. Based on the spectrum we can also understand the energies of electrons ejected by the Compton scattering process (in the region of the Compton peak). According to this spectrum, the ejected electron energies (obtained as $E_f = \omega_1 - \omega_2 - E_B$) are low relative to photoionized electrons for the same energy incident photon.

The impulse approximation may be derived from the A^2 term under the further assumption that the final electron state may be represented by a plane wave. We then have

$$\frac{d^2\sigma}{d\omega_2 d\Omega_2} = \alpha^2\left(\frac{1+cos^2\theta_2}{2}\right)\frac{\omega_2}{\omega_1}\frac{1}{k}J_{n\ell}\,(p_z), \tag{4}$$

where

$$J_{n\ell}\,(p_z) = \frac{1}{2}\int_{p_z}^{\infty} dp\frac{I_{n\ell}\,(p)}{p}. \tag{5}$$

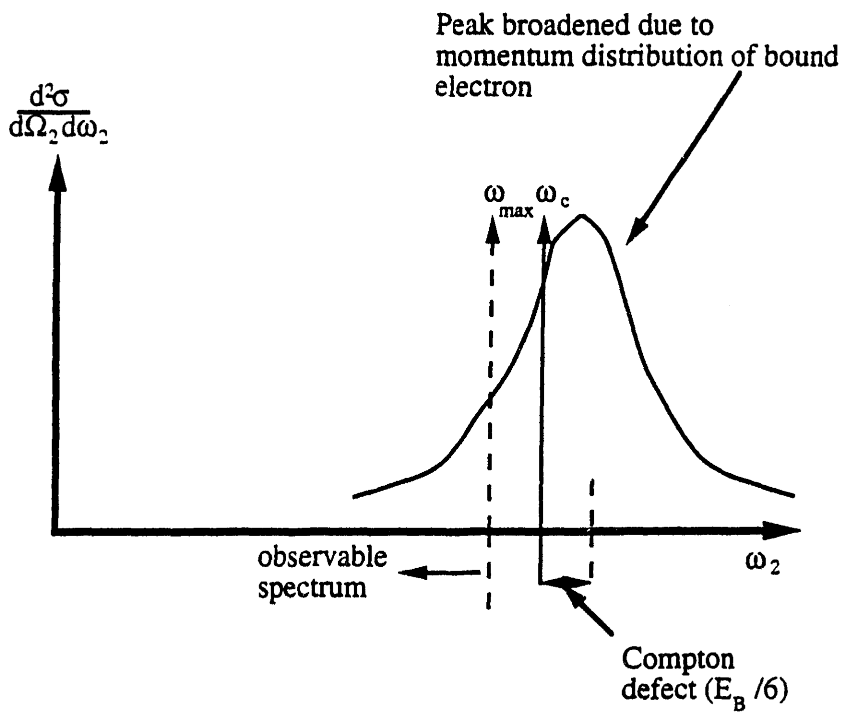

Figure 3. *Cartoon illustrating the kinematic factors that determine the validity of the A^2 approximation.*

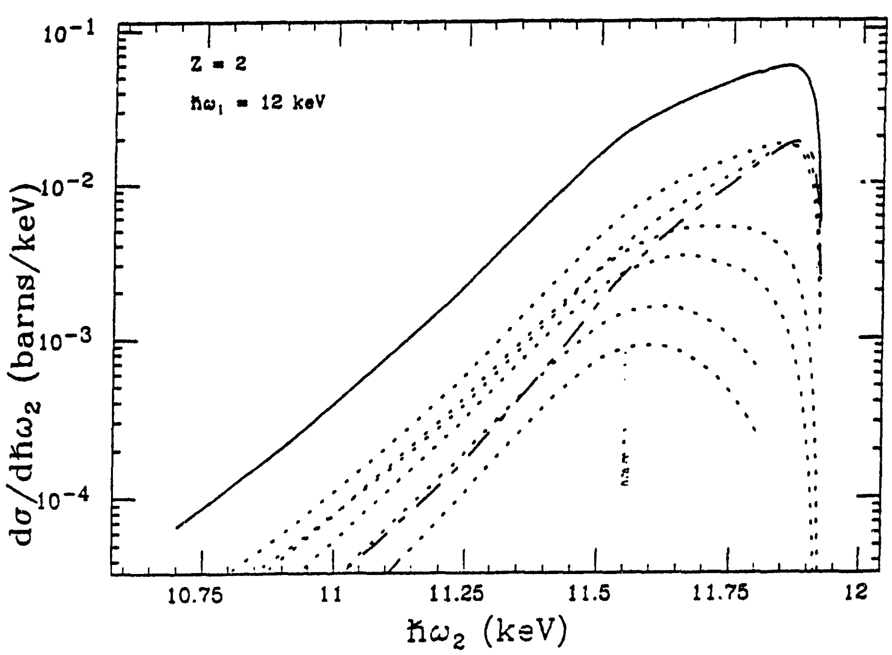

Figure 4. *Scattered photon spectrum for the scattering of 12 keV photons from helium (solid curve). Also shown are the multipole contributions (dots, except at l = 0 is chain dashed curve).*

$J_{nl}(p_z)$ is called the Compton profile of the scattering state with quantum numbers n and l, where

$$p_z = \frac{E_i(\omega_1 - \omega_2) - \omega_1\omega_2(1 - \cos\theta_2)}{k}. \quad (6)$$

This variable is the projection of the momentum of the bound electron on the direction of the photon momentum transfer. Here

$$I_{nl} = |\chi_{nl}(p)|^2 p^2. \quad (7)$$

Tabulations of Hartree-Fock Compton profiles are available for all atoms[10]. In Fig. 5 we present a comparison of a direct evaluation of the A^2 term and the impulse approximation of it to the full S-matrix treatment for the scattering of 8 keV photons from helium. As expected, from Eq. (3), both treatments based on the A^2 term are valid here.

In order to define any cross section for Compton scattering, that has been integrated over scattered photon energies, the question of the soft photon divergence in the **p•A** term must be addressed. The standard program for handling infrared divergences in QED relies on the fact that for sufficiently soft photon energies a divergent radiative process is indistinguishable from a corresponding radiationless process. Therefore, the full amplitude for the radiationless process must be written as the sum of the lowest order amplitude for that process, the amplitudes for radiative corrections to that process and the amplitudes for all radiative processes indistinguishable from the radiationless process. The infrared divergence in the radiative process is cancelled by a corresponding divergence in the radiative corrections to the radiationless process. The radiationless process which corresponds to Compton scattering in the limit of soft scattered photons is photoeffect. Therefore, the full ionization amplitude, which is finite, is written order by order in the fine structure constant as

$$M = M_{pe} + [M_{rc}(\delta) + M_{ird}(\delta)] + \ldots \quad (8)$$

where M_{pe} is the lowest order photoeffect amplitude, M_{rc} are the lowest order radiative corrections to photoeffect, and M_{ird} is the Compton scattering amplitude for scattered photon energies $< \delta$. The full amplitude M must be independent of choice of δ. Gavrila and coworkers[15-19] have evaluated both M_{rc} and M_{ird} and have explicitly demonstrated this cancellation. The effects of this procedure on total photon absorption by hydrogen has recently been investigated by Bergstrom et al[13]. They found that the finite correction of this procedure to the full absorption cross section is small. This means that the total ionization cross section may be accurately approximated by adding the lowest order cross section for photoionization to the A^2 cross section for Compton scattering.

In the A^2 approximation, the singly differential cross-section, observing only the direction but not the energy of the scattered photon is often written in terms of the incoherent scattering factor S(x) (where x is the momentum transfer) as

$$\frac{d\sigma}{d\Omega_2}(\omega_1,\theta_2) = S(x)\left(\frac{d\sigma}{d\Omega_2}\right)_{KN}. \tag{9}$$

Here we have written the cross section in terms of the Klein Nishina cross section for scattering from free stationary electrons

$$\left(\frac{d\sigma}{d\Omega_2}\right)_{KN} = \frac{\alpha^2}{2}\left(\frac{\omega_2}{\omega_1}\right)^2\left\{\frac{\omega_1}{\omega_2}+\frac{\omega_2}{\omega_1}-sin^2\theta_2\right\}. \tag{10}$$

The incoherent scattering factor has been tabulated for all elements by Hubbell et al[21]. Their tabulated values for helium are the configuration interaction calculations of Brown[22] and therefore contain correlation effects. The calculations of Brown are in excellent agreement with the results of Kim and Inokuti[23]; the latter also contain correlation effects, having been obtained from variational wavefunctions. As it is derived by summing over all final states of the system (other than the ground state), the incoherent scattering factor must be understood to include all inelastic scattering process. Compton scattering is the dominant contribution at high photon energies. Another approach to obtain this singly differential cross section (angular distribution) is to integrate an A^2 approximation to the Compton scattering doubly differential cross section over scattered photon energy. In Fig. 6 we present the scattered photon angular distribution calculated within the incoherent scattering factor approximation, and by integrating the doubly differential cross sections obtained within the A^2 and the impulse approximations for the scattering of 10 keV photons from the helium ground state. The incoherent scattering factor is slightly larger than the direct evaluation of the A^2 term, reflecting the contributions of other scattering processes included in the incoherent scattering factor approximation such as Raman scattering, ionization excitation and double ionization. Total cross sections for Compton scattering are then simply obtained by integrating these singly differential cross sections over the scattering angle. The nonrelativistic limit is the classical Thomson cross section.

We have reviewed results pertinent to Compton scattering of keV photons from helium. Simple and acurate methods for calculating cross sections have been given. A discussion of the validity of these approximations has also been presented.

Acknowledgements. I would like to thank the organizers of the workshop and Argonne National Laboratory for the opportunity to attend a very worthwhile event. I also thank those with whom I have investigated the Compton scattering process, Ken-Ichi Hino, Joseph Macek, Richard Pratt, Tihomir Surić and Krunoslav Pisk.

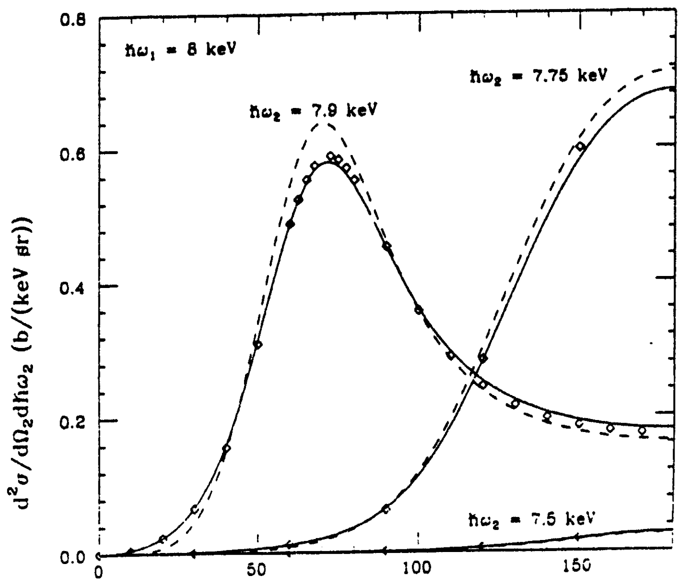

Figure 5. *Comparison of the full A^2 result (solid line) and the impulse approximation with the relativistic it S matrix calculation (diamonds) for the scattering of 8 keV photons from the helium ground state.*

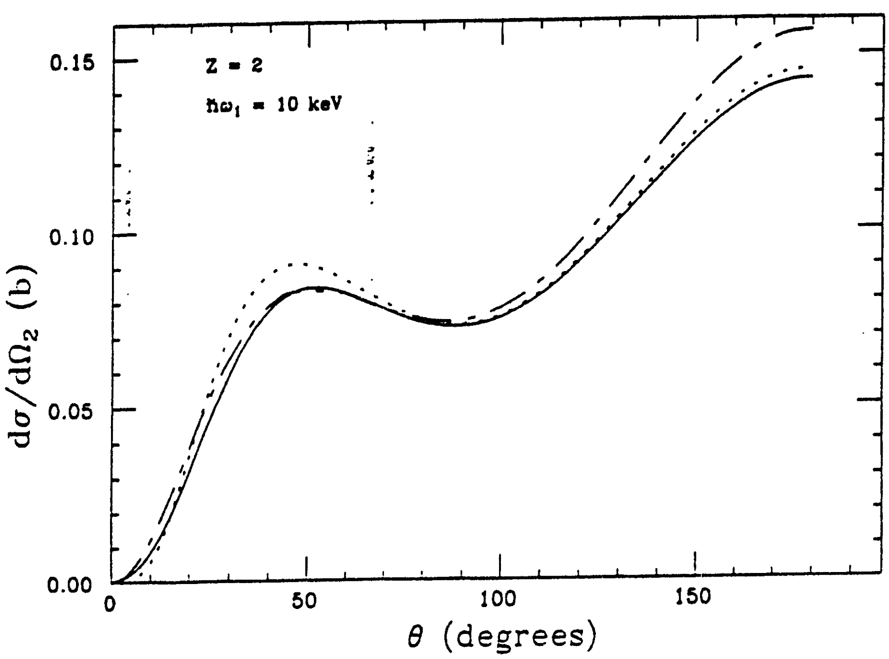

Figure 6. *Comparison of the scattered photon angular distributions for the scattering of 10 keV photons from helium within the incoherent scattering factor (chain dashed curve), A^2 (solid curve), and impulse approximations (dots).*

References

1. James A. R. Samson, Chris H. Greene and R. J. Bartlett, Phys. Rev. Lett. **71**, 201 (1993).
2. J. C. Levin, D. W. Lindle, N. Keller, R. D. Miller, Y. Azuma, N. Berrah Mansour, H. G. Berry, and I. A. Sellin, Phys. Rev. Lett. **67**, 968 (1991); J. C. Levin, I. A. Sellin, B. M. Johnson, D. W. Lindle, R. D. Miller, N. Berrah, Y. Azuma, H. G. Berry and D. -H. Lee, Phys. Rev. **A 47**, R16 (1993).
3. Lars R. Andersson and Joachim Burgdörfer, Phys. Rev. Lett. 71, 50 (1993).
4. Arthur H. Compton, Phys. Rev. 21, 483 (1923); **22**, 409 (1923).
5. P. Debye, Physik. Z. **24**, 161 (1923).
6. J. W. M. DuMond, Phys. Rev. **33**, 643 (1929).
7. P. Eisenberger and P. M. Platzmann, Phys. Rev. **A 2**, 415, (1970).
8. P. Eisenberger and W. A. Reed, Phys. Rev. **B 9**, 3237 (1974).
9. S. Manninen, T. Paakkari, and K. Kajante, Philos. Mag. **29**, 167 (1974).
10. F. Biggs, L. B. Mendelsohn, and J. B. Mann, At. and Nuc.Data Tab. **16**, 201 (1975).
11. Roland Ribberfors, Phys. Rev. **B 12**, 2067 (1975); ibid., 3136 (1975).
12. T. Surić, P. M. Bergstrom, Jr., K. Pisk and R. H. Pratt, Phys. Rev. Lett. **67**, 189 (1991).
13. P. M. Bergstrom, Jr., T. Surić, K. Pisk and R. H. Pratt, Phys. Rev. **A 48**, 1134 (1993).
14. H. A. Kramers and W. Heisenberg, Z. Physik **31**, 681 (1925); I. Waller and D. R. Hartree, Proc. Roy. Soc.(London) **A 124**, 119 (1929).
15. M. Gavrila, Lett. al Nuov. Cim. **5**, 180 (1969); Phys. Rev. **A 6**, 1348 (1972); **A 6**, 1360 (1972); Rev. Roum. Phys. **19**, 473 (1974).
16. A. Costescu and M. Gavrila, Rev. Roum. Phys. **18**, 493 (1973).
17. M. Gavrila and M. N. Tugulea, Rev. Roum. Phys. **20**, 209 (1975).
18. James McEnnan and Mihai Gavrila, Phys. Rev. **A 15**, 1537 (1977).
19. D. J. Botto and M. Gavrila, Phys. Rev. **A 26**, 237 (1982).
20. O. Klein and Y. Nishina, Z. Physik. **52**, 853 (1929).
21. J. H. Hubbell, Wm. J. Veigele, E. A. Briggs, R. T. Brown, D. T. Cromer, and R. J. Howerton, J. Phys. Chem. Ref. Data **4**, 471 (1975).
22. R. T. Brown, J. Chem. Phys. **55**, 353 (1971).
23. Yong-Ki Kim and Mitio Inokuti, Phys. Rev. **165**, 39 (1968).